2021

1D Design and Optimization of a Micro-centrifugal Compressor for an Air Conditioner using R600a

Zhenyuan Mei
University of Maryland, College Park, United States of America

Tao Cao
taocao@umd.edu

Yunho Hwang

1D Design and Optimization of a Micro-Centrifugal Compressor Design for Air Conditioning Applications

Zhenyuan Mei[1], Tao Cao[1*], Yunho Hwang[1]

[1]Center for Environmental Energy Engineering
Department of Mechanical Engineering, University of Maryland,
4164 Glenn Martin Hall Bldg., College Park, MD 20742, United States

*Corresponding author: Tel: (301) 405-8672, email: taocao@umd.edu

ABSTRACT

Miniature compressors play an important role in compact air conditioning systems. Its small size means smaller weight and less material cost. Centrifugal compressors do not have displacement volume and has only one major moving part, which makes it a good candidate for miniature compressor. Typical residential air conditioning systems use R410A as refrigerant due to its good thermodynamic properties and no ozone depletion potential. However, its global warming potential is even higher than that of R22. In addition, it requires high operating speed for a centrifugal compressor. One alternative for R410A is R600a. It has good thermodynamic performance and low impact on environment. Also, its operating pressure is much lower than that of R410A and it requires lower rotational speed. In this paper, a one-dimensional design was performed for a micro-centrifugal compressor for an air conditioning system which has 7 kW cooling capacity and uses R600a as the refrigerant. Furthermore, a single-objective optimization was performed to improve its efficiency using the genetic algorithm. The simulation result shows that the obtained design has 69.7% isentropic efficiency and 2.74 pressure ratio at 250 KRPM.

Keyword: 1D design and optimization, Micro-centrifugal compressor, R600a

1. Introduction

Miniature compressors play an important role in compact air conditioning systems. Its small size means smaller weight and less material cost. Centrifugal compressors do not have displacement volume and has only one major moving part, which makes it a good candidate for miniature compressor. R410A is a refrigerant that has been widely used in residential air conditioning applications due to its good thermodynamic performance and zero ozone depletion potential (ODP). However, its 100-year global warming potential (GWP) is 2,088, which is 15% higher than the GWP of R22 (*IPCC AR4*, 2007; Tian et al., 2015). This means its effect on global warming is about 2,000 times higher than that of carbon dioxide. In addition, it requires high operating speeds for a centrifugal compressor. One alternative to R410A is R600a (isobutane). As a hydrocarbon refrigerant, it is environmentally friendly and has a good thermodynamic performance. Its ODP and GWP are 0 and 5, respectively. And it has large latent heat, which is beneficial for the thermodynamic cycle. Moreover, its operating pressure is relatively lower than that of R410A and it requires lower rotational speed. However, it is highly flammable, which limits its application. Recently, it is gradually being allowed to be used in the refrigerator system with a charge limitation of 150 g. In the future, a compact air conditioner with next generation heat exchangers and compressors may enable its application for residential air conditioning. There have been significant work done on small-scaled centrifugal compressors. Schiffmann et al. (2009) designed a small-scaled centrifugal compressor for a two-stage R134a domestic heat pump system. Its rotational speed was 210,000 RPM, and its peak efficiency was 79%. Javed et al. (2016) designed a two-stage centrifugal compressor for a heat pump system using R134a. Its efficiency at the design point was around 79.5%. Casey et al. (2013) developed a small-scaled centrifugal compressor for a single-stage heat pump using R600. Its rotational speed was 250,000 RPM, and its diameter was around 21 mm. In this paper, preliminary one-dimensional (1D) design and optimization were performed for an air conditioning system using R600a as the refrigerant.

2. Design boundaries

Before performing the preliminary design, it is very important to define the design boundaries. In this paper, the small-scaled centrifugal compressor was designed for a basic four-component vapor compression cycle. The evaporating temperature and condensing temperatures were set to be 10°C and 45°C, respectively. And the cooling capacity was set to be 7 kW. A thermodynamic model was developed in Engineering Equation Solver (EES) to calculate the corresponding refrigerant mass flow rate, suction pressure, and discharge pressure. In this thermodynamic model, it was assumed that there is no pressure drop inside any component. And the maximum isentropic efficiency (85%) from the $n_s d_s$ diagram for single stage compressors from Balje (1981) was used. The suction superheat and condenser subcooling were fixed at 5 K. The calculation result shows that the designed compressor can deliver the refrigerant mass flow rate of 0.025 kg/s at the pressure ratio of 2.74. These values were used as the design boundaries for the centrifugal compressor.

3. 1D centrifugal compressor model and design variables

3.1 1D Compressor Model

In general, there are two types of 1D compressor models (Japikse and Baines, 1994): single zone model and two-zone model. The single zone model assumes the flow inside centrifugal compressor is one-dimensional, and uses a mid-streamline to represent the entire flow passage. And compressor losses are calculated by empirical correlations. Another modeling approach is the two-zone model, which models the flow passage as two zones: the primary zone and the secondary zone. The flow inside the primary zone is considered as an isentropic flow, and the secondary zone consists of low velocity regions such as near wall boundary layer and viscous region which contains substantial losses. The fluid properties of each zone are calculated separately. Eventually, they are mixed at the exit of the impeller, where mixing loss is applied. Japikse (1985) compared the single zone and two-zone models by using the Eckardt compressor. The results show that the deviation of the two-zone model is much less than that of the single zone model. In this paper, the compressor was designed by using the two-zone model in COMPAL®, which is a commercial software developed by NREC. And in our calculation, specific heat polynomial fluid model was used. Where the specific heat of the refrigerant is a function of fluid temperature.

3.2 Rotational Speed

It is important to determine the rotational speed of the centrifugal compressor before designing the compressor. The $n_s d_s$ diagram for single stage compressors from Balje (1981) was used to calculate the estimated rotational speed. Where n_s is the specific speed and d_s is the specific diameter. Note that this diagram was generated for $Re = 2 \times 10^6$ and $s/b_2 = 0.02$, which could be different from the actual design. Therefore, the actual efficiency could be different. According to the $n_s d_s$ diagram, the minimum specific speed required for the maximum efficiency for radial machine was around 0.64, and the corresponding specific diameter was around 4. The calculated rotational speed and impeller diameter were 247 KRPM and 20 mm. In the base design, 240 KRPM was used.

3.3. Incidence Angle

Incidence angle is the difference between the inlet relative flow angle and the inlet blade angle. And it has a positive correlation with the incidence loss (Conrad et al., 1980). In the base design, 1° was used to delay inducer stall as suggested by Javed et al. (2016).

3.4 Hub-to-tip Ratio at Impeller Inlet

The hub-to-tip ratio is defined as the impeller inlet hub radius over the impeller inlet tip radius, which defines the fraction of flow area over the inlet cross-section. This value typically ranges from 0.3 to 0.5 (Javed et al., 2016). Javed et al. (2016) did a parametric study for a similar-sized compressor with the same refrigerant. They found that 0.35 was the optimum value for their compressor. Therefore, in the base design, 0.35 was used.

3.5 Hub Diameter

Many factors affect the minimum hub diameter. For example, the hub diameter needs to be large enough to hold enough blades. Other limiting factors are the minimum shaft diameter required to transport torque and inducer relative Mach number (Javed et al., 2016). Here, the calculation of the minimum shaft diameter required is explained.

Many researchers used aluminum as their impeller material (Javed et al., 2016; Schiffmann and Favrat, 2010) in the past. And in this preliminary design, aluminum 6061 is selected as the material. This minimum diameter is then calculated by the equation derived from Soderberg's failure criteria (Budynas et al., 2011):

$$d = \left(\frac{16n}{\pi}\left\{\frac{1}{S_e}\left[4\left(K_f M_a\right)^2 + 3\left(K_{fs} T_a\right)^2\right]^{0.5} + \frac{1}{S_{yt}}\left[4\left(K_f M_m\right)^2 + 3\left(K_{fs} T_m\right)^2\right]^{0.5}\right\}\right)^{1/3} \quad (1)$$

Where n is the safety factor, and 1.5 was used as the safety factor calculation. $\boldsymbol{S_e}$ is the endurance limit, S_{yt} is the yielding strength, M_a and T_a are the alternating bending moment and alternating torque, M_m and T_m are the midrange bending moment and midrange torque. The calculated minimum diameter was 1.77 mm. Therefore, if the hub inlet diameter was larger than 1.77 mm, it should be able to transport the required torque.

3.6 Number of Blades

Meroni et al. (2018) used an empirical equation from Xu and Amano (2012) to calculate the number of blades required for the impeller as shown in Equation (2). Both equations results were rounded to the closest integer. In this design, the calculated number of blades is 23, which is hard to be fabricated in such a small dimension. Eventually, 14 blades at the impeller exit were used in the base design.

$$N_b = \begin{cases} round(12.03 + 2.544 \times PR_{tt}) & without\ splitter \\ round(-4.527 \times e^{\frac{1.865}{PR_{tt}}} + 32.22) & with\ splitter \end{cases} \quad (2)$$

3.7 Backswept Angle

Nowadays, backswept impeller is widely used since it provides wide surge margin (Boyce, 2003). In the base design, the backswept angle is set to be -45° (Schiffmann and Favrat, 2010).

3.8 Diffuser

There are many types of diffusers. Since in the base design, the impeller is expected to be very small, it is hard to implement a vaned diffuser. Also, the vaneless diffuser usually has a wider operating range. Therefore, the vaneless diffuser was used in this design. The width of the vaneless diffuser was constant and equaled to the impeller exit width, and the ratio of its exit radius over the impeller exit radius was 1.65. After all the design inputs were provided, COMPAL® generated the base compressor design, which has a 2.74 total-to-static pressure ratio and 66% total-to-static efficiency. And the compressor power at the design point was 1.6 kW.

4. DESIGN Optimization

Design optimization was performed to maximize the compressor's efficiency at the design point. Effects on the operating range was not considered during this optimization. Pymoo (Blank and Deb, 2020), which is a genetic algorithm optimization package available in Python, was used. And since the current problem was a single objective optimization, the basic genetic algorithm was used. The problem formulation is shown below:

$$\begin{aligned} & \mathrm{f} = -\eta_{is,ts} \\ s.t. \quad & no\ stall\ or\ choke \\ & 0.9 - r_{1h} \leq 0 \end{aligned} \quad (3)$$

A Python script was written to bridge Pymoo and COMPAL®. The objective function is essentially the compressor design software whose outputs are η , and other important design parameters. Because the solver solves the

minimization problem, a minus sign is added to the calculated efficiency to convert it into a minimization problem. There are five design variables, and their ranges are listed in Table 1.

Table 1: Range of design variables.

Design variables	I_{1t}	r_{1h}/r_{1t}	β_{2b}	N	r_5/r_{2t}
Unit	degree	-	degree	KRPM	-
Lower bound	-2.0	0.3	-50	200	1.05
Upper bound	2.0	0.5	0	250	2.00

The population size was 50. Objective space tolerance was used as the stopping criteria. The average change in the objective space should be less than 10^{-5} to stop the solver. For better robustness, the maximum value in the last 50 generations was picked. Note that this stopping criterion was evaluated every 10th generation.

Three optimization runs were performed. The initial values were selected randomly. The best fitness values of each generation for each run are shown in Figure 1. Because of the stopping criteria, the number of generations for each run is different. Eventually, all three runs yield a similar result.

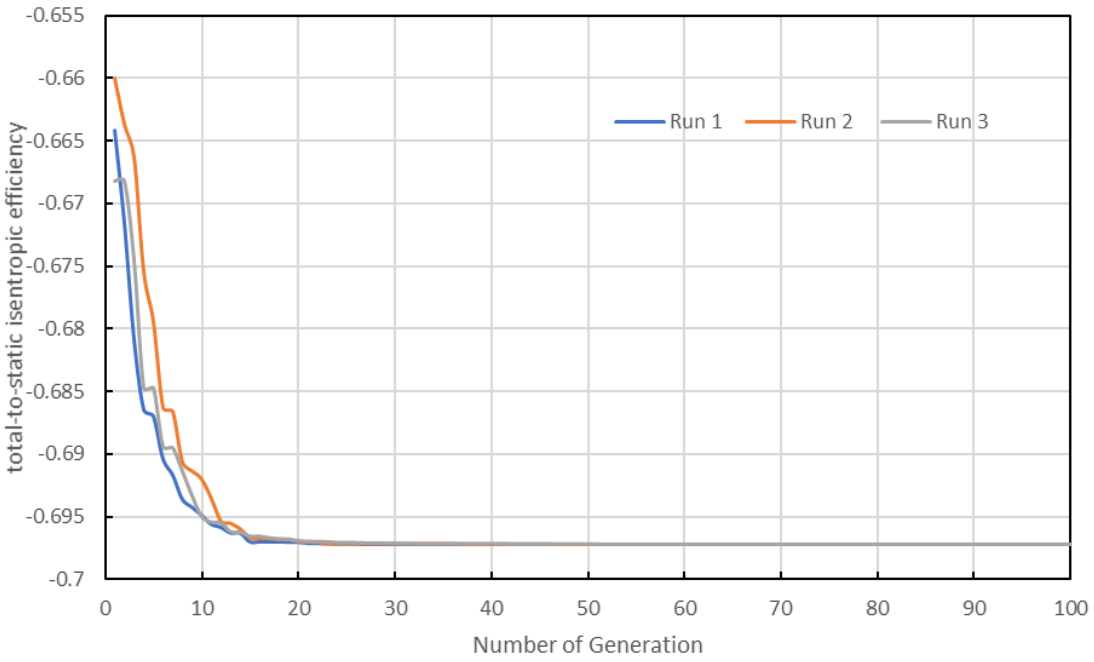

Figure 1: Optimization calculation history.

The comparison between the base design and optimized design is shown in Table 2. The optimized design had a smaller inlet hub-to-tip ratio, and the incidence angle was 2°. Moreover, a higher rotational speed was required for the optimized design. The total-to-static isentropic efficiency was improved by 3.5, from 66.2% to 69.7%.

Table 2: Comparison between the base design and the optimized design.

Parameters	**Base design**	**Optimized design**
Number of main blades	7	7
Number of splitter blades	7	7
Inlet tip blade angle	-52.3°	-50.6°
Inlet hub-to-tip ratio	0.35	0.30
Impeller outlet blade angle	-45°	-50°
Impeller outlet radius	12 mm	11 mm

Impeller exit width	0.6 mm	0.7 mm
Impeller diffuser radius	19 mm	22 mm
Design speed	240 KRPM	250 KRPM
Total-to-static efficiency	66.2%	69.7%

Figure 2 and Figure 3 show the compressor maps of the base and optimized design. The compressor performance maps were generated by varying the fraction of compressor speed from 0.6 to 1.0 with an interval of 0.2. Furthermore, 1.1 times design speed was also added to check its off-design performance at a higher speed.

In general, the optimized design has a higher efficiency than the base design. Especially when the refrigerant mass flow rate and compressor speed are low, which could be the part-load condition. Also, the base design shows a sharp efficiency drops when the refrigerant mass flow rate increases, but the optimized design shows a more flattened shape. In addition, it may be noticed that the optimized design has a narrow operating range as compared to the base design. Overall, the optimized design has a narrower operating range when its speed is high but has higher efficiency, especially in the low-speed region.

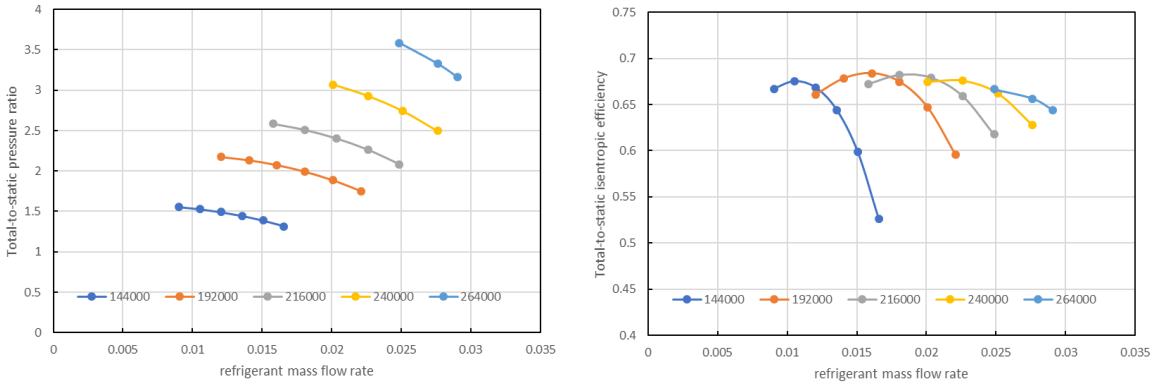

Figure 2: Compressor performance map - base design: (left) pressure ratio, (right) efficiency.

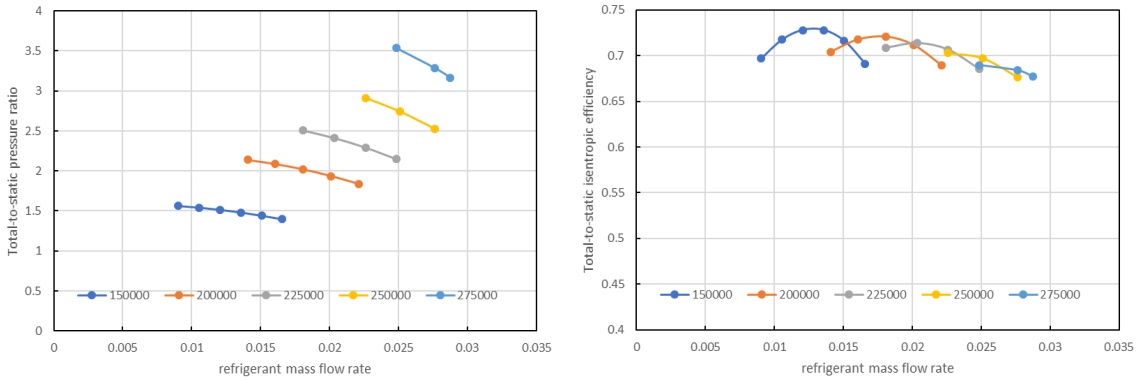

Figure 3: Compressor performance map - optimized design: (left) pressure ratio, (right) efficiency.

5. Conclusions

In conclusion, a 1D design was performed for a small-scale centrifugal compressor for air conditioning systems. A genetic algorithm was used to optimize the centrifugal compressor design. The final 1D design has an 11 mm radius. It reaches 69.7% total-to-static isentropic efficiency at design speed of 250 KRPM. Its total-to-static pressure ratio is 2.74. The low isentropic efficiency is probably due to limited compressor rotational speed and relatively large relative tip clearance due to a small dimension. For future work, it is necessary to conduct 3D CFD simulations to evaluate the compressor's performance in depth and followed by experimental evaluations.

Nomenclature

d_s	specific diameter, $\frac{D\Delta h^{0.25}}{\sqrt{\dot{Q}_{in}}}$	(-)
Δh	adiabatic head	(kJ/kg)
GWP	Global Warming Potential	(-)
I	incidence angle	(°)
KRPM	thousand revolution per minute	(-)
ODP	Ozone Depletion Potential	(-)
PR	pressure ratio	(-)
$\dot{Q}_{in}$	impeller inlet volumetric flow rate	(m^3/s)
r	radius	(mm)
Re	Reynold number	(-)
s	tip clearance	(mm)
S_e	endurance limit	(MPa)
S_{yt}	yielding strength	(MPa)
T	torque	(Nm)
M	bending moment	(Nm)
N_b	number of blades	(-)
n	safety factor	(-)
n_s	specific speed, $\frac{\omega\sqrt{\dot{Q}_{in}}}{\Delta h^{0.75}}$	(-)
β	blade angle	(°)
η	efficiency	(-)
ω	impeller rotational speed	(rad/s)

Subscript

$1h$	impeller inlet hub
$1t$	impeller inlet tip
a	alternating
m	midrange
ts	total-to-static
Tt	total-to-total
is	isentropic

Reference

AR4 Climate Change 2007. (2007). IPCC. https://www.ipcc.ch/report/ar4/wg1/

Balje, O. E. (1981). *Turbomachines-A guide to design, selection, and theory*. John Wiley & Sons.

Blank, J., and Deb, K. (2020). pymoo: Multi-objective Optimization in Python. *ArXiv:2002.04504 [Cs]*. http://arxiv.org/abs/2002.04504

Boyce, M. P. (2003). *Centrifugal compressors: A basic guide*. PennWell.

Budynas, R. G., Nisbett, J. Keith., and Shigley, J. Edward. (2011). *Shigley's mechanical engineering design* (9th ed.). McGraw-Hill; WorldCat.org.

Casey, M. V., Krähenbuhl, D., and Zwyssig, C. (2013). The Design of Ultra-High-Speed Miniature Centrifugal Compressors. *European Conference on Turbomachinery Fluid Dynamics and Thermodynamics ETC*, *10*, 1–13.

Conrad, O., Raif, K., Wessels, M., and Aktiengesellschaft, D.-B. (1980). THE CALCULATION OF PERFORMANCE MAPS FOR CENTRIFUGAL COMPRESSORS WITH VANE-ISLAND DIFFUSERS. *Proceedings of the Twenty-Fifyh Annual International Gas Turbine Conference and Exhibit*, 14.

Japikse, D. (1985). Assessment of Single- and Two-Zone Modeling of Centrifugal Compressors, Studies in Component Performance: Part 3. *Volume 1: Aircraft Engine; Marine; Turbomachinery; Microturbines and Small Turbomachinery*, V001T03A023. https://doi.org/10.1115/85-GT-73

Japikse, D., and Baines, N. C. (1994). *Introduction to Turbomachinery*. Oxford: Oxford University Press.

Javed, A., Arpagaus, C., Bertsch, S., and Schiffmann, J. (2016). Small-scale turbocompressors for wide-range operation with large tip-clearances for a two-stage heat pump concept. *International Journal of Refrigeration*, *69*, 285–302. https://doi.org/10.1016/j.ijrefrig.2016.06.015

Meroni, A., Zühlsdorf, B., Elmegaard, B., and Haglind, F. (2018). Design of centrifugal compressors for heat pump systems. *Applied Energy*, *232*, 139–156. https://doi.org/10.1016/j.apenergy.2018.09.210

Schiffmann, J., and Favrat, D. (2009). Experimental investigation of a direct driven radial compressor for domestic heat pumps. *International Journal of Refrigeration*, *32*(8), 1918–1928. https://doi.org/10.1016/j.ijrefrig.2009.07.006

Schiffmann, J., and Favrat, D. (2010). Design, experimental investigation and multi-objective optimization of a small-scale radial compressor for heat pump applications. *Energy*, *35*(1), 436–450. https://doi.org/10.1016/j.energy.2009.10.010

Tian, Q., Cai, D., Ren, L., Tang, W., Xie, Y., He, G., and Liu, F. (2015). An experimental investigation of refrigerant mixture R32/R290 as drop-in replacement for HFC410A in household air conditioners. *International Journal of Refrigeration*, *57*. https://doi.org/10.1016/j.ijrefrig.2015.05.005

Xu, C., and Amano, R. S. (2012). Empirical Design Considerations for Industrial Centrifugal Compressors. *International Journal of Rotating Machinery*, *2012*, 15. https://doi.org/10.1155/2012/184061

ACKNOWLEDGEMENT

We gratefully acknowledge the support of the Center for Environmental Energy Engineering (CEEE) at the University of Maryland.